Progress in Organic Coatings 111 (2017) 267–272

Contents lists available at ScienceDirect

Progress in Organic Coatings

journal homepage: www.elsevier.com/locate/porgcoat

Ion probe techniques to measure the distribution of substrate elements in coatings for copper alloys

Rosie Grayburn[a,*], Zachary E. Voras[b], Christopher M. Goodwin[b], Ming-Chang Liu[c], Thomas P. Beebe Jr.[b], Alan Phenix[a]

[a] Getty Conservation Institute, 1200 Getty Centre Drive, Suite 700, Los Angeles, CA, USA
[b] Department of Chemistry and Biochemistry, University of Delaware, Newark, DE, USA
[c] Department of Earth, Planetary and Space Sciences, UCLA, Los Angeles, CA, USA

ARTICLE INFO

Keywords:
Corrosion inhibitor
Depth profiling SIMS
Acrylic coatings

ABSTRACT

Copper can have a beneficial or unfavorable effect on coating performance, depending on the additives present in the formulation. The distribution of copper was studied in acrylic coating formulations on brass substrates with and without benzotriazole to gain insights into the role of copper ions. Using depth profiling secondary ion mass spectrometry it was found that on ageing copper migrated from the coating towards the substrate in the presence of benzotriazole, possibly due to inhibition at the coating-metal interface. However, closer inspection by ToF-SIMS shows an even distribution of BTA in the coating and no evidence of inhibition via complexation or chemisorption on the metal surface.

1. Introduction

The presence of copper ions in coatings can be constructive or destructive. On one hand, copper ions can interact with additives to inhibit corrosion [1], while on the other hand it has also been reported that copper ions can alter the properties of the polymer coating [2–4], for example causing chemical degradation. How do we decide whether the action of copper ions is of cause for concern?

The additive to be investigated in this work is benzotriazole (BTA). BTA is a commonly used copper corrosion inhibitor against a variety of pollutants, for example anthropogenic gases [5–7], aqueous chlorides [8–10] and acidic media [11,12]. While it is employed as a corrosion inhibitor in a wide range of industries (e.g. power, water, oil), BTA is often used in the stabilization of copper-based artefacts [13,14], especially for the treatment of chloride corrosion (also known as “bronze disease”). It was originally suggested using electrochemical methods and infrared spectroscopy that chelation of copper ions with a lone pair of electrons on the azole ring leads to a linear polymeric Cu(I)-BTA complex formation [15,16], formed during immersion of copper in a near-neutral solution of BTA. The production and transport of soluble copper ions from the metal was found to be the determining factor for growth of this structure. An alternative surface structure, elucidated by surface sensitive techniques, ellipsometry and molecular modelling, is simply chemisorption of BTA onto the copper surface [9,17,18]. The structure of the surface depends on the pH [8,19], oxidation of the copper substrate [20] and BTA concentration [21]. However, the complex interplay of these factors makes it difficult to predict the structure and in turn the inhibitor performance.

BTA is a mixed-type inhibitor, as it has been found to retard metal oxidation as well as cathodic processes. The barrier properties of either chemisorbed or complexed surface structure can explain the performance of the BTA-inhibited surface compared to bare metal [8]. A dual layer system has been confirmed by ellipsometry and electrochemical methods whereby polymeric Cu(I)-BTA forms on top of the initial chemisorbed layer [17,22,23]: using a rotating-disk electrode the chemisorbed layer was found to be the most resistive whereas the Cu(I)-BTA complex was found to be porous [23]. Specifically regarding chloride corrosion, BTA was shown to complex alternately with chloride and copper [24], thus preventing a chloride-induced catalytic reaction.

The inhibition and structure of BTA on copper alloy has been mostly studied using immersion treatment in hot, dilute solution [25,26] or impregnation under vacuum [27]. However, BTA is often incorporated into coating formulations as an anti-corrosion additive and for its UV absorption properties [28,29]. For example, Incralac is an acrylic coating made up of Paraloid™ B44, benzotriazole, a carrier solvent and levelling agent [30]. Paraloid™ B44 is a methylmethacrylate (MMA) copolymer, which has been found to contain MMA, ethyl acrylate (EA) and *n*-butyl methacrylate (BMA) in a 70:28:1 ratio [31,32]. Incralac was developed in the 1960′s to satisfy demand for a long-lasting treatment for the protection of copper. It has been widely used since then for the conservation of copper and bronze outdoor works of art

* Corresponding author.Current affiliation and contact details: Department of Conservation, Winterthur Museum, 5105 Kennett Pike, Winterthur, DE, USA; rgrayb@winterthur.org

http://dx.doi.org/10.1016/j.porgcoat.2017.06.016
Received 8 December 2016; Received in revised form 9 March 2017; Accepted 7 June 2017
Available online 14 June 2017
0300-9440/

with some inconsistency in positive reports of performance [33].

In order to further investigate the mechanism of BTA and the involvement of copper within coatings on copper alloys, depth profiling was carried out using secondary ion mass spectrometry (SIMS). Static SIMS is an ion probe technique used to study surface composition to parts-per-billion resolution [34]. Dynamic SIMS has been used to study polymer composition and properties in depth resolution [35–37], but has less often been utilized to measure substrate element distribution in polymers [38]. Poly(methyl methacrylate) (PMMA) on silicon or glass has been studied extensively due to this system's use in the semiconductor industry: the ingress of elements from these inert substrates has been reported as negligible [39]. In this study, elemental depth profiles from aged coatings on a copper alloy could be matched with Time-of-Flight (ToF)-SIMS images to cross-reference molecular features from a coating cross-section.

2. Materials and methods

2.1. Depth profiling

Samples were cut from Commercial Bronze sheet (90 Cu:10 Zn, McMaster-Carr, USA) to 7 × 7 cm squares. (The Commercial Bronze alloy is classed as a brass [40], and will be referred to as such in the remainder of the paper.) Prior to coating, the surface was mechanically polished to a mirror finish with silicon carbide paper (P1200 Grit), followed by alumina (0.1 μm, aqueous dispersion) on a MicroCloth (all Buehler, Germany). The samples were then rinsed with DI water and ultrasonically cleaned in ethanol for 60 min [41].

Samples were spin-coated (Chemat Technology, Inc.) with a 4 mL aliquot of the coating (Table 1) at 500 rpm (10 s) then 2.5 krpm (60 s) to achieve a 1.5 ± 0.1 μm thick coating. Thickness was measured using a Multimode IV atomic force microscope equipped with a J-type piezo (Veeco Metrology Group, Santa Barbara, CA). Silicon tips from Bruker were used in tapping mode (Bruker Inc., Billerica, MA). Samples were aged artificially in an Atlas Ci4000 Weather-O-meter® (ISO 4892-2:2013; filtered xenon arc UV-B: 340 nm; cycle: 102 min light at 65 °C and 18 min condensation; irradiance: 60 W/m^2) for 72, 240 and 720 h then cut to 1 cm^2 diameter using a cleaned metal die. Samples were left to dry for 24 h then coated with gold to assist in sample surface charge compensation during the SIMS depth profile.

Depth profiling was carried out at the UCLA-NSF National Ion Microprobe Facility, UCLA on the Cameca 1290 SIMS instrument by using a mass-filtered $^{16}O^-$ beam, with an impact energy of 23 KeV (−13 KeV at the source and +10 KeV at the sample) and an ion current of 10 nA. Secondary ions were collected with the axial electron multiplier (EM) under mass resolution (M/ΔM) of ~2000.

2.2. ToF-SIMS

Samples were aged artificially (as described above) for 720 h then cut to 1 cm^2 diameter using a cleaned metal die.

Analysis was carried out on a TOF-SIMS IV system (upgraded to TOF-SIMS V capabilities) (ION-TOF GmbH; Münster, Germany) at the Surface Analysis Facility in the Department of Chemistry and Biochemistry, University of Delaware. Measurements were performed in high-current bunched-mode using the 25-keV Bi_3^+ cluster with a pre-bunched pulse-width of 640 ps and a measured target current of 0.3 pA. Images were collected to the static SIMS limit with a pixel density of 128 × 128 pixels; all secondary ions were extracted with ± 2 kV into the TOF mass analyzer and given a 10 kV post-acceleration for detection. A low energy electron flood gun was used for charge compensation allowing samples to be imaged without a coating of gold. ToF-SIMS images were taken on the edge of a crater sputtered using a 4 kV Ar_{2000}^+ gas cluster ion beam (GCIB).

Table 1
Coating formulation for samples analysed by depth profiling SIMS and ToF-SIMS. Coating 1 is an imitation Incralac [30]; coating 2 is an imitation Incralac minus the anti-corrosion additive BTA.

Ingredients (manufacturer)	Coating 1	Coating 2
Paraloid™ B44 (Dow, USA)	17 g	17 g
Benzotriazole (TCI, Japan)	0.25 g	–
Toluene (Merck, USA)	100 mL	100 mL
Paraplex® G-60 (Hallstar, USA) [Epoxidised Soybean Oil]	1.7 g	1.7 g

3. Results and discussion

3.1. Depth profiling

Depth profiling was carried out on aged and unaged coated brass samples to measure the distribution of elements within the polymer. Subsequently, the coating thickness was measured to inform depth profile analysis. Both aged and unaged coats were found to be (1.6 ± 0.3) μm thick.

It is important to consider factors which could have implications for analysis of depth profiles due to the depth resolution uncertainties. For example, it has been found on analogous samples that the experimental error of SIMS crater depth measurements can be ± 15% [38]. This is due to the properties of organic polymers and their susceptibility to chemical or physical changes that may be caused by implantation of the primary ion beam and sputtering [39,42–46]. For example beam damage in a similar polymer, PMMA, has been characterized as main chain scission and side-chain loss [47].

Fig. 1 shows a depth profile of unaged coating 1 on a brass substrate. The intensities of the secondary ions are shown in counts per second. The depth of the coating is approximated to sputtering time: from 0 to 4000 s the beam etches from the coating surface towards the metal substrate. The primary ion beam intensity of 10 nA at 23 keV would only deposit 0.23 mW onto the samples surface, and the resulting temperature change is negligible. Data at < 1 cps have a high signal-to-noise due to Poisson statistics.

A range of isotopes was investigated using depth profiling: ^{63}Cu, ^{64}Zn, ^{12}C and ^{16}O. Nitrogen, although present in the coating additives, could not be detected due to the use of the $^{16}O^-$ ion beam. Copper and zinc make up the metal substrate so an increase in Cu and Zn signal denotes approaching coating-metal interface. Fig. 1 shows a sharp increase in copper and zinc signals at 1000 s indicating that the ion beam is approaching the metal surface in depth, but also that the substrate elements are detected in the coating before ageing. After this sharp

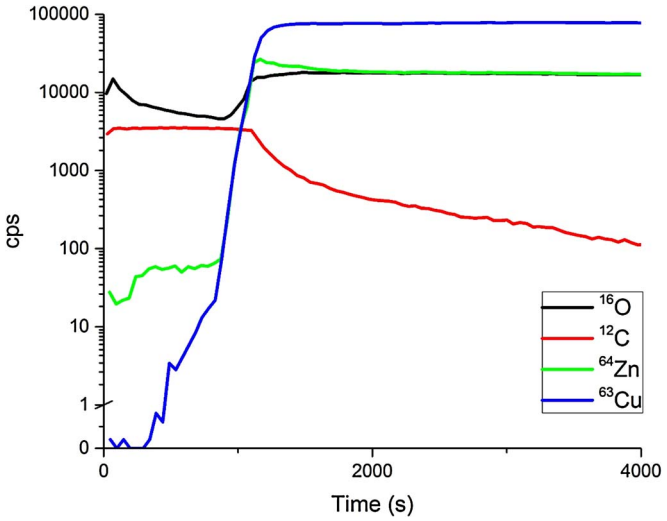

Fig. 1. Depth profile of unaged coating 1 on a brass substrate. The counts per second from four isotopes were analysed during a 4000 s measurement.

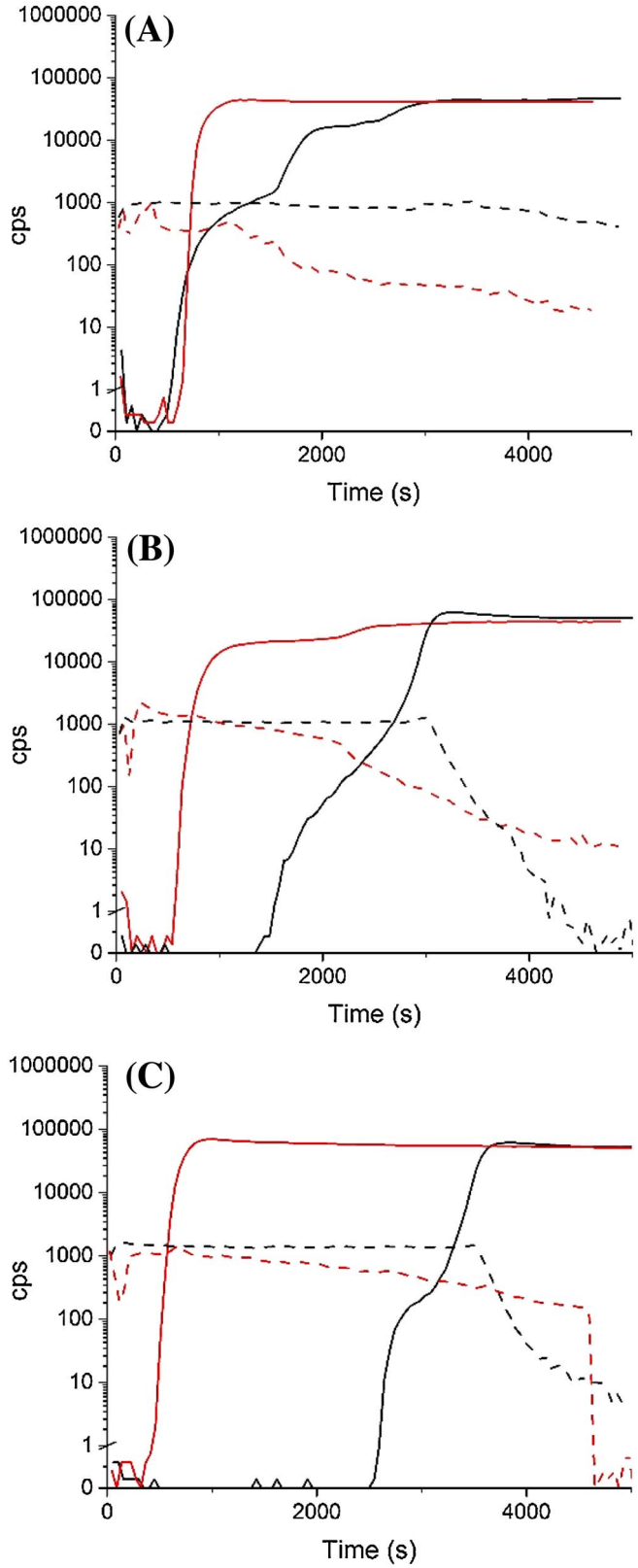

Fig. 2. Copper (solid line) and carbon (dotted line) depth profiles of coating 1 (black) and coating 2 (red) artificially aged (A) 72, (B) 240 and (B) 720 h. (For interpretation of the references to colour in this figure legend, the reader is referred to the web version of this article.)

increase, the Cu and Zn signals plateau as a results of the ion beam penetrating into the homogenous metal substrate. Carbon and oxygen are the major elements in the coating so the C and O signals can infer the thickness of the coating and polymer properties. From time 0–1000 s the carbon signal remains flat as the beam sputters the homogenous coating. A flat carbon signal has previously been attributed to the random orientation of copolymer molecules [35]. At 1000 s, where the Cu and Zn signals increase, the carbon signal drops off – carbon traces in the metal could be a result of impurity in the alloy. The oxygen signal decreases from 0 to 1000 s due to the oxidation of the coating [48] possibly caused by damage to the acrylic [42]. At the coating-metal interface the signal increases then plateaus possibly due to a reaction of the oxide on the metal surface.

Substrate elements have been shown in Fig. 1 to have similar depth profiles. However, subsequent analyses of depth profiles focus on the copper and carbon signals only in order to further investigate the involvement of copper within aged coatings on copper alloys.

Fig. 2 shows the carbon and copper profiles from aged coating 1 and 2 on a brass substrate. The aged coating 1 data shows a gradual shift in the onset of copper profiles on ageing. The coating-substrate interface characterized by the copper/carbon crossover is at 3000–3500 s for all aged coating 1 samples. Compared to the unaged coating (Fig. 1) the onset remains at 500 s but the interface is measured at 1100 s, which suggests a change in coating properties on ageing. Sputter rates for coating 1 are 10.7 ± 1.7 nm^3/ion and 1.7 ± 0.1 nm^3/ion for the unaged and aged respectively.

After 72 h artificial weathering there is a stepwise increase of copper from the coating to the brass interface from 500 s. The curve flattens out at 3000 s as the primary ion beam interacts with the brass only. After 240 h artificial ageing there is no copper found in the coating until 1500 s after which a gradual increase in copper signal from 0 to 80000 cps occurs during 2000 s. After 720 h artificially ageing, there is no copper detected in the coating until 2500 s. On ageing, the slope of the copper profiles for coating 1 also increases from the point of onset to plateau. The shift in copper profile onset suggests that on application of the coating, copper ions are dispersed some nanometers into the coating (Fig. 1) and that on ageing copper ions migrate from the coating to the brass surface. The migration of copper in an analogous substrate (PMMA) has been attributed to several phenomena [49]: 1) traces of acid could cause copper salt or soap formation leading to migration, 2) interchain alignment allows copper to travel through the polymer matrix, and 3) Cu (II) interaction with electric field gradients. It has also been suggested that changes in polymer structure could affect the diffusion of copper ions [50]. Therefore it is possible that the shift in copper profile on ageing is a reflection of structural polymer degradation during artificial ageing [36,51]. The shift is unlikely to be due to ion-induced degradation because PMMA has been found to be more susceptible to chemical changes in the beam than structural alterations [44].

The carbon profiles of coating 1 samples aged 240 and 720 h show a decrease in signal to zero at the coating-substrate interface as copper (and zinc) replaces the coating. The same behavior is not observed with the least aged sample nor the unaged sample (Fig. 1): at the perceived interface, the carbon signal stays level and does not decrease steeply as the beam reaches the metal.

Depth profiles for coating 2 on a brass substrate do not show significant change with ageing. Copper profiles for these coats increase sharply from 0.1–80,000 cps at 500 s followed by a plateau, which suggests a) a very clear coating-metal interface and b) that no copper is present in the coating. Carbon profiles show a sharp dip after 100 s, followed by a slow decrease in intensity – the clear coating-substrate interface observed in Fig. 1 is not present. This could be due to ion-induced damage accumulation which is not removed by the primary ion beam [46,52].

If the copper-carbon profile crossover is indicative of the coating-substrate interface, Fig. 2 shows that the sputter rate is much faster into coating 2 than the coating 1. This suggests that the BTA in coating 1 also improves the stability of the layer in the ion beam, which could be caused by increased coating stability due to additional hydrogen

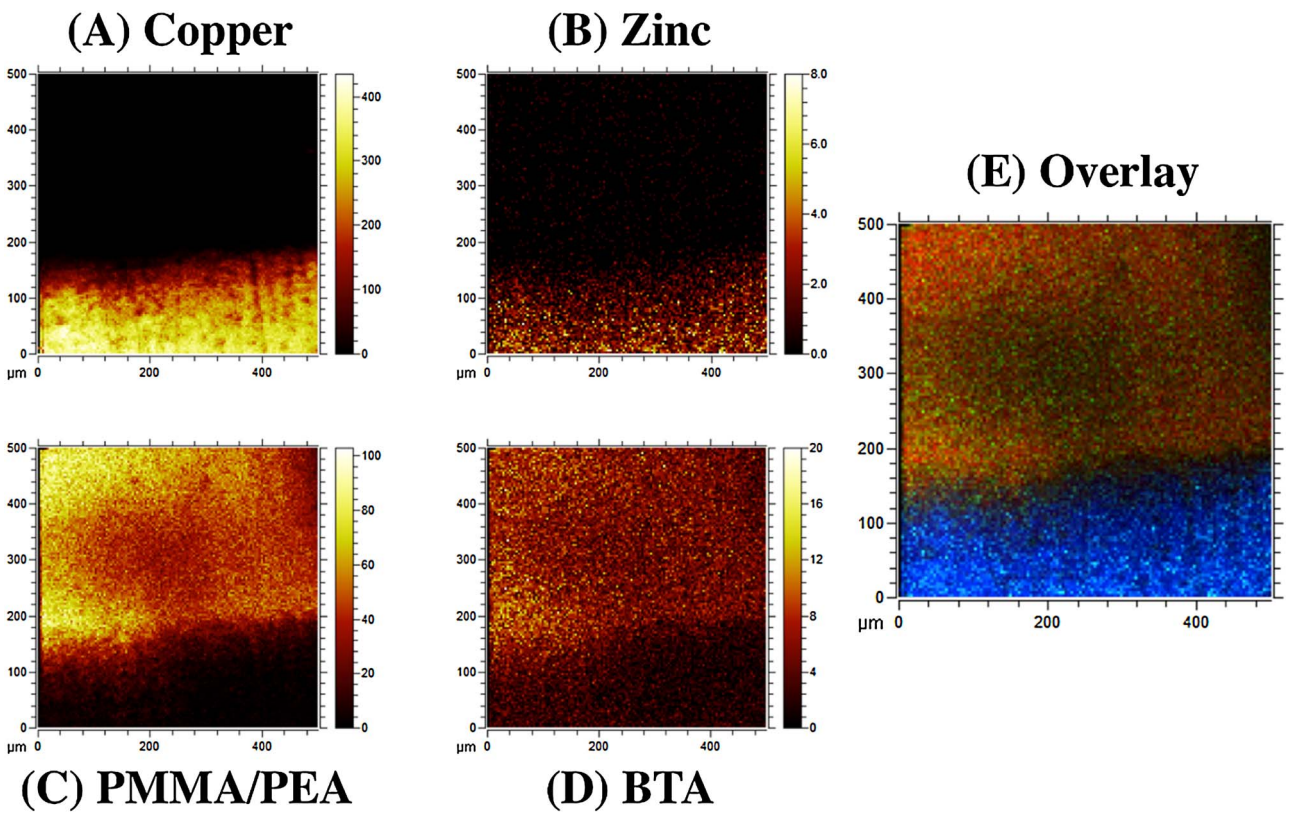

Fig. 3. ToF-SIMS images of an aged spin-cast film cross-section of coating 1 on a brass coupon formed by sputtering with a GCIB (see Experimental section for details). (A) is the copper image as an addition of Cu^+ and $^{65}Cu^+$ mass fragment images. (B) is the zinc image as an addition of Zn^+ and $^{66}Zn^+$ mass fragment images. (C) is the acrylic image as an addition of $C_2H_3O_2^+$, $C_2H_5O^+$, and $C_3H_5O_2^+$ mass fragment images. (D) is the BTA image as an addition ofNH_4^+ N_2^+, $C_6H_5N_2^+$, and $C_6H_4N_3^+$ mass fragment images. (E) is an overlay of images (A) through (D) with the following color channels: (A) blue, (B) cyan, (C) red, (D) green. (For interpretation of the references to colour in this figure legend, the reader is referred to the web version of this article.)

bonding between BTA and the acrylic [53].

As shown in Table 1, benzotriazole is found in coating 1 only. Therefore the difference in depth profiles could be attributed to the presence of this anti-corrosion additive. The coating containing BTA has a lower sputtering time than without. It was also found that coating 1 depth profiles show a migration of copper from the coating to the metal interface on ageing. This could be due to Cu-BTA complex formation at the copper surface creating a copper ion concentration gradient. It has been shown the concentration of BTA determines if the Cu-BTA complex is formed; at the concentration shown in Table 1, BTA is known to complex with copper in solution [21]. The results of the complex formation phenomena have been observed with solid phase chemistry when evaluating the coating's performance [54]. However, with this depth profiling technique we cannot differentiate between Cu and Cu-BTA in the coating.

Migration of copper in the presence of BTA on ageing has been shown using depth profiling SIMS. By using ToF-SIMS imaging, BTA distribution in an aged coating is further investigated to deduce whether it remains dispersed in the dried resin, is found mostly at the coating-metal interface and whether it is occurring in a complexed Cu-BTA form.

3.2. Time-of-Flight SIMS

ToF-SIMS was employed in order to see if the copper ingress observed in depth profiling of aged films could be attributed to formation of the Cu-BTA complex. Prior to ToF-SIMS measurements, expected peaks were elucidated from earlier work. Notoya measured the ToF-SIMS signals from copper immersed in BTA [55]. It was found that Cu-BTA complexes exist in oligomers with up to 5 monomers (positive ion beam) or 3 monomers (negative ion beam) of BTA. In addition, BTA which remains uncomplexed to copper can form CN^-, C_3N^-, $C_6H_4N^-$ and $C_6H_4N_3^-$ ions. MMA and ethyl acrylate (EA) fragments should be recognizable from the Paraloid™ resin which makes up the bulk of the coating. The most recognizable features come from the side groups of the MMA and EA monomers ($C_2H_3O_2^+$ and $C_3H_5O_2^+$ respectively) [56,57]. However, the ions of the acrylic resin measured can vary according to ion source and dose [39].

Fig. 3 shows the ToF-SIMS images for individual coating components (A–D) and the overlaid images (E). The coating-metal interface is clearly evidenced by the copper signal. The zinc signal is lower than the copper, as expected for this alloy (also Fig. 1). Both metals show a decrease in signal prior to the interface. Synchronously, an observed drop in acrylic molecular signal is present at the acrylic-brass interface. This is in line with the observations made in Fig. 2 for the same sample: the steep copper depth profile close to the coating-metal interface infers less copper in the coating than younger coatings. Fig. 3(D) shows that BTA molecules are dispersed throughout the coating after ageing. There is no clear increase in BTA concentration at the coating-metal interface, as one would expect from proposed inhibition mechanisms for the inhibitor [1]. However, the images show BTA mass fragments are detected on top of the copper and zinc signals, which could suggest complexation or chemisorption. That said, no definitive copper-BTA molecular fragments were measured; thus the Cu-BTA complex was not positively identified on the coating-metal interface nor dispersed within the coat. This could be due to the instability of the Cu-BTA complex under these experimental conditions or the relatively low concentration of the expected Cu-BTA in comparison to previous literature that investigated the complex [55].

4. Conclusions

The distribution of copper ions through aged acrylic coatings was measured using depth profiling SIMS in order to gain an understanding of the protective mechanism with or without the addition of benzotriazole. General trends were observed because quantitative measurements are difficult when measuring elements within polymers using this technique [38]. In the coating containing BTA, copper ions migrated out of the coating towards the coating-copper interface which implied the formation of a Cu-BTA protective layer, a mechanism also suggested when BTA is applied to a metallic substrate via immersion [1]. Conversely, the copper depth profile did not change when a coating omitting BTA was aged which implies no copper migration.

ToF-SIMS imaging was employed to locate the inhibitive Cu-BTA complex. We are not able to measure definitive copper-BTA molecular fragments expected at the interface possibly due to the instability or concentration of the complex during measurement. Nevertheless, an even dispersion of BTA within the coating was measured. This could have the effect of increasing absorption of damaging UV light [48,58] which can also improve the performance of the coating.

The $^{16}O^-$ ion source used for the depth profiling SIMS does not allow for detection of N. If a Cs^+ beam has been utilized, CN^- would have been detected but Cs^+ is a much heavier ion and would have caused greater sample damage. Although the very low primary ion beam current did not induce much temperature change on the surface, beam damage and polymer degradation caused by ion bombardment was unavoidable and possibly reduced the depth resolution of the measurements. However, the higher impact energy was necessitated by the fact that higher energy primary ions were needed to measure the copper signal.

While this work has focused on the protective properties of a conservation coating, ongoing work looks at the detrimental substrate effects of copper on the acrylic. It has been reported that copper ions or salts can have a degradative effect on polymer coatings, by causing film thinning through promoting thermal oxidative degradation [4] or acting as a catalyst for radical production [2]. Future work will therefore apply depth profiling of pure polymer coatings on copper and pre-corroded surfaces, which can be more easily cross-referenced to molecular damage signals from corresponding ToF-SIMS data.

Acknowledgements

We thank Professor Kevin McKeegan (UCLA) for the use of the Cameca 1290 SIMS instrument. The UCLA ion microprobe facility is partially supported by a grant from the NSF Instrumentation and Facilities program. The authors would like to acknowledge the NSF (9724307) and the NIH NIGMS COBRE (P30-GM110758) programs for support of the Surface Analysis Facility at the University of Delaware. The reviewers are thanked for their insightful comments.

References

[1] M. Finšgar, I. Milošev, Inhibition of copper corrosion by 1,2,3-benzotriazole: a review, Corros. Sci. 52 (2010) 2737–2749.
[2] D.L. Allara, C.W. White, R.L. Meek, T.H. Briggs, Mechanism of oxidation at a copper–polyethylene interface. II. Penetration of copper ions in the polyethylene matrix, J. Polym. Sci. 14 (1976) 93–104.
[3] L.S. Korugic-Karasz, E.A. Hoffmann, Polymer ion implantation: present and future prospects, Nonlinear Opt. Quant. Opt. 32 (2004) 135–140.
[4] M.C. Burrell, J. Fontana, J.J. Chera, Study of the enhanced oxidative degradation of polymer films at polymer/copper (oxide) interfaces using depth profile and inert marker techniques, J. Vac. Sci. Technol. A 6 (1988) 2893–2896.
[5] C. Fiaud, N. Ghimouz, Inhibitive effect of benzotriazole on atmospheric corrosion of copper in presence of hydrogen sulphide, Br. Corros. J. 24 (1989) 279–283.
[6] F.M. Al-Kharafi, B.G. Ateya, Effect of sulfides on the electrochemical impedance of copper in benzotriazole-inhibited media, J. Electrochem. Soc. 149 (2002) B206–B210.
[7] T.M. Christensen, N.R. Sorensen, Thermal stability of benzotriazole on copper during atmospheric corrosion, Surf. Interface Anal. 17 (1991) 3–6.
[8] I.C.G. Ogle, G.W. Poling, Corrosion inhibition of copper with benzotriazole, Can. Metall. Q. 14 (1975) 37–46.
[9] F. Mansfield, T. Smith, E.P. Parry, Benzotriazole as corrosion inhibitor for copper, Corrosion 27 (1971) 289–294.
[10] I.D. MacLeod, Conservation of corroded copper alloys: a comparison of new and traditional methods for removing chloride ions, Stud. Conserv. 32 (1987) 25–40.
[11] H. Hassairi, L. Bousselmi, S. Khosrof, E. Triki, Evaluation of the inhibitive effect of benzotriazole on archeological bronze in acidic medium, Appl. Phys. A 113 (2013) 923–931.
[12] R. Walker, Benzotriazole as a corrosion inhibitor for immersed copper, Corrosion 29 (1973) 290–298.
[13] H. Brinch Madsen, A preliminary note on the use of benzotriazole for stabilizing bronze objects, Stud. Conserv. 12 (1967) 163–167.
[14] V.C. Sharma, U.S. Lal, T. Singh, Method for stabilization of leaded bronzes affected by corrosion of lead, Stud. Conserv. 48 (2003) 203–209.
[15] I. Dugdale, J.B. Cotton, An electrochemical investigation on the prevention of staining of copper by benzotriazole, Corros. Sci. 3 (1963) 69–74.
[16] G.W. Poling, Reflection infra-red studies of films formed by benzotriazole on Cu, Corros. Sci. 10 (1970) 359–370.
[17] V. Brusic, M.A. Frisch, B.N. Eldridge, F.P. Novak, F.B. Kaufman, B.M. Rush, G.S. Frankel, Copper corrosion with and without inhibitors, J. Electrochem. Soc. 138 (1991) 2253–2259.
[18] M. Finšgar, J. Kovač, I. Milošev, Surface analysis of 1-hydroxybenzotriazole and benzotriazole adsorbed on Cu by X-ray photoelectron spectroscopy, J. Electrochem. Soc. 157 (2010) C52–C60.
[19] R. Youda, H. Nishihara, K. Aramaki, Sers and impedance study of the equilibrium between complex formation and adsorption of benzotriazole and 4-hydroxybenzotriazole on a copper electrode in sulphate solutions, Electrochim. Acta 35 (1990) 1011–1017.
[20] R.F. Roberts, X-ray photoelectron spectroscopic characterization of copper oxide surfaces treated with benzotriazole, J. Electron Spectrosc. Relat. Phenom. 4 (1974) 273–291.
[21] G. Lewis, Adsorption isotherm for the copper-benzotnazole system, Br. Corros. J. 16 (1981) 169–171.
[22] J.J. Kester, T.E. Furtak, A.J. Bevolo, Surface enhanced raman scattering in corrosion science: benzotriazole on copper, J. Electrochem. Soc. 129 (1982) 1716–1719.
[23] R. Alkire, A. Cangellari, Effect of benzotriazole on dissolution of copper in the presence of fluid flow: I. Experimental, J. Electrochem. Soc. 136 (1989) 913–919.
[24] T. Hashemi, C.A. Hogarth, The mechanism of corrosion inhibition of copper in NaCl solution by benzotriazole studied by electron spectroscopy, Electrochim. Acta 33 (1988) 1123–1127.
[25] F. Ammeloot, B. Millet, C. Fiaud, L. Robbiola, E.M.M. Sutter, Characterization of Naturally Grown Oxide Layers on Copper with and Without Benzotriazole by Electrochemical and Photoelectrochemical Measurements, in: I.D. MacLeod, S.L. Pennec, L. Robbiola (Eds.), Earthscan Ltd., London; United Kingdom, 1997, pp. 95–98.
[26] C. Sease, Benzotriazole: a review for conservators, Stud. Conserv. 23 (1978) 76–85.
[27] H.B. Madsen, Further remarks on the use of benzotriazole for stabilizing bronze objects, Stud. Conserv. 16 (1971) 120–122.
[28] G. Bierwagen, T.J. Shedlosky, K. Stanek, Developing and testing a new generation of protective coatings for outdoor bronze sculpture, Prog. Org. Coat. 48 (2003) 289–296.
[29] J.E. Fagel, G.W. Ewing, The ultraviolet absorption of benzotriazole1a, J. Am. Chem. Soc. 73 (1951) 4360–4362.
[30] N.R. Bharucha, M.T. Baker, Clear Lacquers for Copper and Copper Alloys: A Summary of Research Carried out by British Non-Ferrous Metals Research Association for International Copper Research Association, British Non-Ferrous Metals Research Association, London, 1965.
[31] O. Chiantore, M. Lazzari, Characterization of acrylic resins, Int. J. Polym. Anal. Charact. 2 (1996) 395–408.
[32] C.V. Horie, 8 – acrylic resins, in: C.V. Horie (Ed.), Materials for Conservation, Butterworth-Heinemann, 1987, pp. 103–112.
[33] J. Wolfe, R. Grayburn, H. Khanjian, A. Heginbotham, A. Phenix, Decronstructing Incralac: A Formulation Study of Acrylic Coatings for the Protection of Outdoor Bronze Sculpture, Preprints of ICOM-CC 2017, 2017.
[34] A. Benninghoven, F.G. Rüdenauer, H.W. Werner, Secondary Ion Mass Spectrometry: Basic Concepts, Instrumental Aspects, Applications, and Trends, J. Wiley, New York, 1987.
[35] V.R. Deline, G. COulon, T.P. Russell, D.C. Miller, SIMS and copolymer ordering, in: A. Benninghoven (Ed.), Secondary Ion Mass Spectrometry, Sims VII Wiley, Hyatt Regency Hotel, Monterey, California, USA, 1990, pp. 359–362.
[36] S.E. Harton, F.A. Stevie, D.P. Griffis, H. Ade, SIMS depth profiling of deuterium labeled polymers in polymer multilayers, Appl. Surf. Sci. 252 (2006) 7224–7227.
[37] S.E. Harton, F.A. Stevie, Z. Zhu, H. Ade, Carbon-13 labeled polymers: an alternative tracer for depth profiling of polymer films and multilayers using secondary ion mass spectrometry, Anal. Chem. 78 (2006) 3452–3460.
[38] R.G. Wilson, G.E. Lux, C.L. Kirschbaum, Depth profiling and secondary ion mass spectrometry relative sensitivity factors and systematics for polymers/organics, J. Appl. Phys. 73 (1993) 2524–2529.
[39] D. Briggs, I. Fletcher, Cs+ ion beam damage of poly (vinyl chloride) and poly (methyl methacrylate) studied by high mass resolution ToF-SIMS, Surf. Interface Anal. 25 (1997) 167–176.
[40] C22000 copper alloy data, Properties of Wrought and Cast Copper Alloys, Copper Development Association Inc., 2017.
[41] A. Elia, K. De Wael, M. Dowsett, A. Adriaens, Electrochemical deposition of a copper carboxylate layer on copper as potential corrosion inhibitor, J. Solid State Electrochem. 16 (2012) 143–148.

[42] D. Briggs, M.J. Hearn, Interaction of ion beams with polymers, with particular reference to SIMS, Vacuum 36 (1986) 1005–1010.
[43] S.J. Simko, D.P. Griffis, R.W. Murray, R.W. Linton, Dose-dependent cesium ion beam damage effects on chemically modified poly(methyl methacrylate) films using secondary ion mass spectrometry and x-ray photoelectron spectroscopy, Anal. Chem. 57 (1985) 137–142.
[44] G.J. Leggett, J.C. Vickerman, Effects of damage during the SIMS analysis of poly (vinyl chloride) and poly(methyl methacrylate), Appl. Surf. Sci. 55 (1992) 105–115.
[45] I. Gilmore, M. Seah, Static SIMS: a study of damage using polymers, Surf. Interface Anal. 24 (1996) 746–762.
[46] M.S. Wagner, G. Gillen, Impact energy dependence of SF5+ ion beam damage of poly(methyl methacrylate) studied by time-of-flight secondary ion mass spectrometry, Appl. Surf. Sci. 231–232 (2004) 169–173.
[47] B. Pignataro, M.E. Fragalà, O. Puglisi, AFM and XPS study of ion bombarded poly (methyl methacrylate), Nucl. Instrum. Methods Phys. Res. Sect. B 131 (1997) 141–148.
[48] O. Chiantore, M. Lazzari, Photo-oxidative stability of paraloid acrylic protective polymers, Polymer 42 (2001) 17–27.
[49] E.L. Kern, G. Eierman, E.G. Bobalek, S.M. Skinner, Migration of copper through high purity poly(methyl methacrylate), J. Appl. Polym. Sci. 2 (1959) 253–254.
[50] J. Crank, G.S. Park, Diffusion in high polymers: some anomalies and their significance, Trans. Faraday Soc. 47 (1951) 1072–1084.
[51] O. Chiantore, L. Trossarelli, M. Lazzari, Photooxidative degradation of acrylic and methacrylic polymers, Polymer 41 (2000) 1657–1668.
[52] C.W.T. Bulle-Lieuwma, W.J.H. van Gennip, J.K.J. van Duren, P. Jonkheijm, R.A.J. Janssen, J.W. Niemantsverdriet, Characterization of polymer solar cells by TOF-SIMS depth profiling, Appl. Surf. Sci. 203–204 (2003) 547–550.
[53] D. Bougeard, N. Le Calvé, B.S. Roch, A. Novak, 1,2,4-Triazole: vibrational spectra, normal coordinate calculations, and hydrogen bonding, J. Chem. Phys. 64 (1976) 5152–5164.
[54] L.B. Brostoff, Coating Strategies for the Protection of Outdoor Bronze Art and Ornamentation, Van't Hoff Institute for Molecular Sciences (HIMS), Universiteit van Amsterdam, Amsterdam The Netherlands, 2003 pp. 180.
[55] T. Notoya, M. Satake, T. Ohtsuka, H. Yashiro, M. Sato, T. Yamauchi, D. Schweinsberg, Structures of metal-benzotriazole films on copper and other metals, J. Corros. Sci. Eng. 6 (2003) C076.
[56] T. Learner, Analysis of Modern Paints, Getty Publications, 2004.
[57] D. Briggs, M.J. Hearn, B.D. Ratner, Analysis of polymer surfaces by SIMS. 4—a study of some acrylic homo- and co-polymers, Surf. Interface Anal. 6 (1984) 184–192.
[58] J. Keck, H.E. Kramer, H. Port, T. Hirsch, P. Fischer, G. Rytz, Investigations on polymeric and monomeric intramolecularly hydrogen-bridged UV absorbers of the benzotriazole and triazine class, J. Phys. Chem. 100 (1996) 14468–14475.